TÜBİTAK

Turkish Journal of Physics

http://journals.tubitak.gov.tr/physics/

Research Article

Turk J Phys
(2021) 45: 90 – 104
© TÜBİTAK
doi:10.3906/fiz-2012-8

$\psi(2S)$ and J/ψ production in pp collisions at $\sqrt{s}$ = 7, 8 and 13 TeV

Yasir ALI[1], Uzma TABASSAM[1,*], Syed Uzair AHMED SHAH[1], Atif ARIF[1], Mais SULEYMANOV[2] Zain UL ABIDIN[1]

[1]Department of Physics, COMSATS University Islamabad, Park Road, Islamabad, Pakistan
[2]Institute for Physical Problem, Baku State University, Baku, Azerbaijan

Received: 16.12.2020 • **Accepted/Published Online:** 16.03.2021 • **Final Version:** 29.04.2021

Abstract: Proton-proton collision is an essential part of high energy physics, as it is a baseline for nucleus-nucleus and hadron-nucleus collisions. Quark-gluon plasma, an exotic state of strongly interacting QCD matter, is routinely produced in heavy nuclei high-energy collisions. Charmonium, the bound states of $c\bar{c}$ produced at the early stages of collisions, are nice probes to examine the properties of matter through which they pass. The differential cross-sections of inclusive $\psi(2S)$ in pp collisions at energies of $\sqrt{s}$ = 7, 8 and 13 TeV have been studied. PYTHIA 8.1 event generator is used for the simulation of data. The differential cross-section of inclusive J/ψ is also presented in order to examine the $\psi(2S)$ to J/ψ ratio at similar energies. Both charmonium states are simulated in dimuon ($\mu^+\mu^-$) decay channel. The simulated data is also compared with the ALICE and LHCb experimental data based at LHC. We have plotted the differential cross-section as a function of transverse momentum (p_T) and rapidity y. PYTHIA simulation is found to be in good agreement with ALICE data for low p_T interval, y interval close to midrapidity, while PYTHIA agrees with LHCb data at low p_T interval. It is observed that the LHCb differential cross-section distributions of J/ψ and $\psi(2S)$ as a function of y are lower compared to the ALICE data distributions and PYTHIA simulations. The $\psi(2S)$ to J/ψ ratio is also well explained by PYTHIA and shows an increase in production of inclusive J/ψ as compared to inclusive $\psi(2S)$.

Key words: Quark-gluon plasma, charmonium, differential cross-section, transverse momentum, PYTHIA

1. Introduction

The charmonium production in heavy ion collision plays an important role to understand the nonperturbative aspect of quantum chromodynamics (QCD) [1–3]. Due to heavy mass, the bound state $c\bar{c}$ is believed to be nonrelativistic, thus provides us another way to look for an additional aspect of QCD theory [4–6]. The mechanisms of charmonium production are a two-step process, first step is the hard partonic interactions with large momentum transfer (described by means of perturbative quantum chromodynamics) which results in the initial $c\bar{c}$ pair production. In the second step, the bound state $c\bar{c}$ is evolved through soft processes which can be described by nonperturbative QCD. Thus, charmonium give new insight into the interplay between soft and hard production mechanisms [7, 8].

Three effective thermodynamical models used to describe the production mechanism of charmonium states are the color singlet model, color evaporation model and color octent model. Although charmonia have been studied extensively, their production mechanism is still not fully understood. Measurements in

*Correspondence: uzma.tabassam@comsats.edu.pk

pp collisions at the highest LHC energies can provide further information regarding prompt charmonium production, contributing to a deeper understanding of the corresponding production processes [9, 10].

Due to different binding energy of $\psi(2S)$, it is supportive to study the J/ψ and it may also be useful for the evaluation of the medium temperature. Thus the ratio of these charmonium states provides an important information about recombination mechanism [11]. While J/ψ production is a probe of the hot and dense medium created in ultrarelativistic heavy ion collisions [12–14], and is sensitive to nuclear effects. J/ψ is not related to the creation of cold nuclear matter effects, such as parton distribution modification functions [15, 16]. To measure the hot and cold medium effects, a detailed study of $\psi(2S)$ production in the absence of a nucleus is required. In this regard, pp collision provides a baseline for the heavy ion collisions to quantify the nuclear effects [17].

The current analysis is based on the study of the production of two states of charmonium i.e. $\psi(2S)$ and J/ψ in pp collision over a rapidity region of $2.5 < y < 4$. The transverse momentum (p_T) and rapidity (y) distributions have been obtained using the PYTHIA 8 Monte Carlo simulation code and data is compared with the ALICE [18–20] and LHCb [21–23] experiments at LHC. The energy dependence of the spectra at $\sqrt{s}$ = 7, 8 and 13 TeV have been analyzed.

2. Methodology

In this article, we have studied the inclusive $\psi(2S)$ and J/ψ production in proton-proton (pp) collisions at the center-of-mass energies of $\sqrt{s}$ = 7, 8 and 13 TeV in forward rapidity region ($2.5 < y < 4$) as a function of the transverse momentum (p_T) and rapidity (y) in dimuon ($\mu^+\mu$) decay channel. The inclusive $\psi(2S)$ to J/ψ cross-section ratio is also be studied at $\sqrt{s}$ = 7, 8 and 13 TeV as a function of p_T and y. The study is based on simulation data, which is generated using Monte Carlo event generator, PYTHIA 8. The $\psi(2S)$ and J/ψ is forced to decay in dimuon channel by externally handling the decay mode in order to regenerate the experimental condition.

The PYTHIA 8 is a QCD inspired model which is developed for event generation process [24]. The significant feature of the PYTHIA code is multiparticle production by the multitude of different processes implemented at different stages of pp collision. Perturbative interactions in pp collisions occur between the partons, which are carried out in the framework of multiparton interactions (MPI) [25]. About four to ten partonic interactions (PI) are occur in a single event which depends on the impact parameter of pp collision [26]. The perturbative interactions are accompanied by initial state radiation and final state radiation. The partons created in MPIs are connected via strings. Color reconnection (CR) of partons from different partonic interactions establish a connection by rearranging themselves and thus reduce the total length of string, which decrease the total multiplicity [27]. The hadronization is carried out by Lund String fragmentation model [28]. As separation between partons increases, the energy stored in string increases linearly with it due to color confinement. The string breaks when energy is enough to produce an additional $q\bar{q}$ pair, each of which is connected through a short string. The process will continue until very small pieces of strings are remain. All these processes contribute in the final yield of charmonium.

3. Results and discussion

ALICE and LHCb experiments based at LHC CERN play major contributions in measuring the production cross-section of $\psi(2S)$ and J/ψ states at different energies. The present analysis is focused on the study of the

production cross-sections of $\psi(2S)$ and J/ψ as a function of p_T and y in dimuon decay channel in pp collisions at $\sqrt{s} = 7$, 8 and 13 TeV in forward rapidity region of $2.5 < y < 4$, using PYTHIA 8 model and its comparison with the data from the ALICE [18–20] and LHCb [21–23] experiments.

3.1. $\psi(2S)$ resonance at $\sqrt{s} = 13$ TeV

Figure 1 depicts the distributions of differential cross-section of inclusive $\psi(2S)$ production as a function of p_T from PYTHIA 8 model simulations and data obtained from ALICE and LHCb experiments. These distributions are plotted in the p_T interval of 016 GeV/c. About 10 million pp events are generated using PYTHIA 8 for the $\psi(2S)$ distribution. The bottom panel shows the ratio of the yields of the data obtained from the model to the experimental data. There observed 3 regions for the p_T distributions: in region I $p_T < 1$ GeV/c the model's prediction is higher than both of the distributions of experimental data. After that it seems that the model can describe well the experimental data in the interval of $1 < p_T < 4$ GeV/c. Then the simulation model underestimates the experimental data in the region of $4 < p_T < 8$ GeV/c (region II). From the bottom panel it seems that the ratio decreases in this region. For $p_T > 8$ GeV/c (region III) the values of the ratios decrease slowly with p_T. Again the model underestimates the experimental data distributions.

Figure 2 shows the differential cross-section of inclusive $\psi(2S)$ production as a function of y in the interval of 2.54. Five million pp events are generated for the $\psi(2S)$ distribution. The simulated distribution is compared with the ALICE and LHCb data obtained from [18] and [21], respectively. The bottom panel shows the ratio of the yields for the simulated data to the experimental data distributions. The behavior of the ratio of the yields indicates two y regions with: $y < 3.1$ and $y > 3.1$. In region I ($y < 3.1$) the model can describe the ALICE data but in region II ($y > 3.1$) with y the model predictions are lower than the ALICE experimental data. While for the whole y interval LHCb data distribution is lower than ALICE data and the PYTHIA simulated distribution.

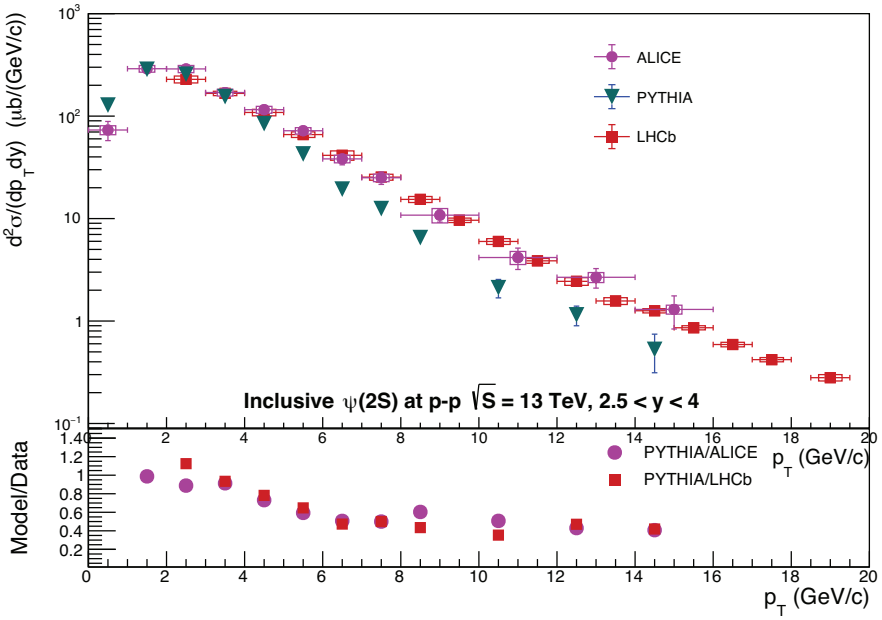

Figure 1. The p_T distribution for the differential cross-section of $\psi(2S)$ production in pp collisions at $\sqrt{s} = 13$ TeV.

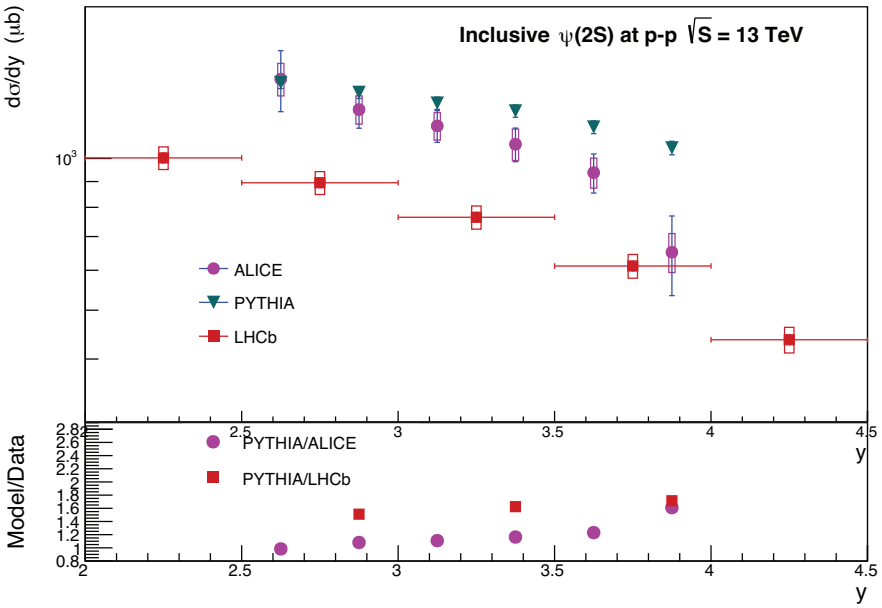

Figure 2. The y distribution for the differential cross-section of $\psi(2S)$ production in pp collisions at $\sqrt{s}$ = 13 TeV.

In this section, we show the differential cross-section of inclusive J/ψ production in pp collision at $\sqrt{s}$ = 13 TeV and forward rapidity range of $2.5 < y < 4$. The differential cross-section as a function of p_T and y is studied using PYTHIA code, and compared with ALICE data [18] in the p_T interval of $0 < p_T < 30\ GeV/c$. In Figure 3, the differential cross-section of inclusive J/ψ production as a function of p_T is shown in p_T from 030 GeV/c. Ten million pp events are generated for the J/ψ distribution. The simulated differential cross-section is compared with the ALICE [18] and LHCb[21] data. Again the bottom panel shows the ratio of the yields for data coming from the model to the data from the experiments. One can see that the code can explain well the ALICE and LHCb experimental data in the interval of $p_T < 4\ GeV/c$ (the ratio is around 1). While for the interval of 48 GeV/c, the deviation between experimental distributions and model started which increases with p_T. The model underestimates both the experimental distributions for $p_T > 4\ GeV/c$. In the p_T interval of 48 GeV/c the ratios decrease sharply with p_T. Then in the interval of $p_T \simeq 8 - 21\ GeV/c$, the values of the ratio decrease slowly and data is almost constant in the interval of $p_T \simeq 21 - 28\ GeV/c$. Figure 4 shows the distributions of the differential cross-section of J/ψ production as a function of y in the interval of $y = 2.54.5$ (the bottom panel shows the ratio of the yields for data obtained from the model and experiments). Five million pp events are generated for J/ψ distribution. The simulated differential cross-section is compared with the data obtained by ALICE and LHCb collaborations. The model can describe well the ALICE data in the interval of $2.5 < y < 3.1$. Out of the interval the code overestimate the ALICE experimental data. While for the whole y interval LHCb data distribution is lower than PYTHIA and ALICE data distributions.

3.2. Ratio of $\psi(2S)$ to J/ψ cross-section at $\sqrt{s}$ = 13 TeV

The ratio of inclusive cross-sections of $\psi(2S)$ production to ones for J/ψ productions as a function of p_T at $\sqrt{s}$ = 13 TeV is shown in Figure 5 and as a function of y in Figure 6. The ratio distributions are obtained from PYTHIA 8 simulation code. Apparently for the case of the ratio of inclusive cross-sections as a function of p_T

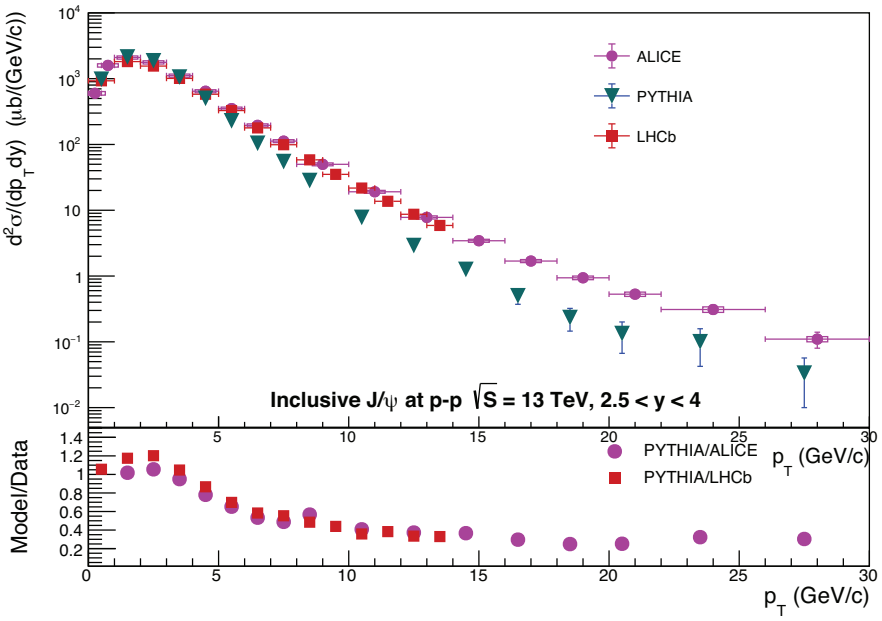

Figure 3. The p_T distributions for the differential cross-section of $\psi(2S)$ production in pp collisions at $\sqrt{s}$ = 13 TeV.

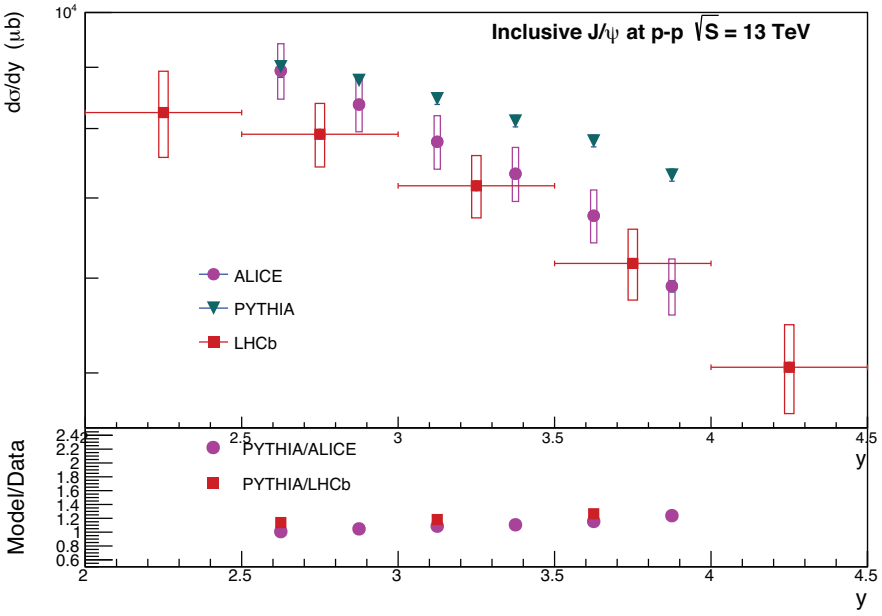

Figure 4. The y distributions for the differential cross-section of $\psi(2S)$ production in pp collisions at $\sqrt{s}$ = 13 TeV.

simulated results are in good agreement with ALICE and LHCb results. When the distribution is plotted as a function of y (Figure 6) LHCb distribution is lower again as compared to ALICE data and PYTHIA simulated data. It is very interesting to note that the ratios for the p_T distributions increase linearly with p_T though the ratios almost does not depend on y.

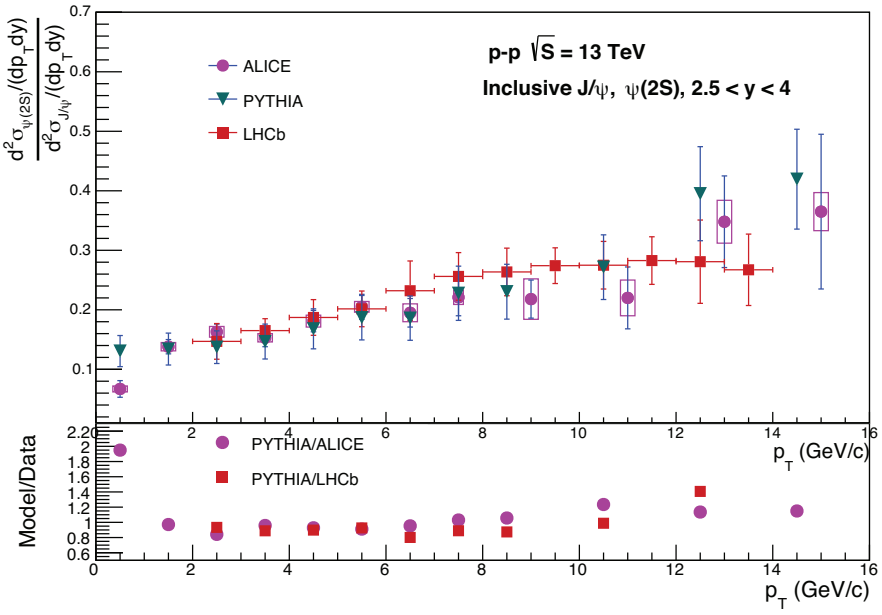

Figure 5. The p_T dependence of ratios for the differential cross-sections of $\psi(2S)$ productions to ones for the J/ψ productions.

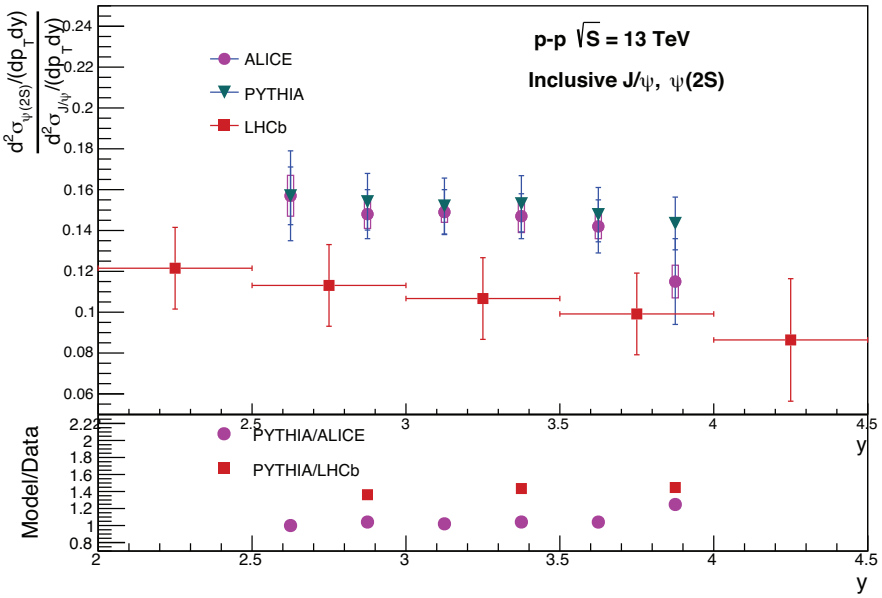

Figure 6. The y dependence of ratios for the differential cross-sections of $\psi(2S)$ productions to ones for the J/ψ productions.

3.3. $\psi(2S)$ resonance at $\sqrt{s} = 8$ TeV

In Figure 7, the differential cross-section of $\psi(2S)$ is shown in p_T from 012 GeV/c. Ten million events have been simulated for $\psi(2S)$. The differential cross-section distribution obtained from simulated result is compared with the published ALICE [19] measurements (the bottom panel shows the ratio of the yields for data obtained

from model and experiment). One can see that there are 3 p_T regions for the behavior of the ratio: in region I of $p_T < 3.0\ GeV/c$, the ratio does not depend on p_T and is 1, good prediction from the model; in region II at the values of $p_T = 3 - 5$, the ratio decreases; in region III at the values of $p_T > 5\ GeV/c$, the ratio is around 0.5. In Figure 8, differential cross-section of $\psi(2S)$ is presented in y bins from 2.54. Five million pp events are generated for $\psi(2S)$. The simulated result is compared with the measurement performed by ALICE collaboration (the bottom panel shows the ratios of the yields of data obtained from the model and the experiment). Evidently the model can describe the experimental behavior of the yield for the most of the p_T region.

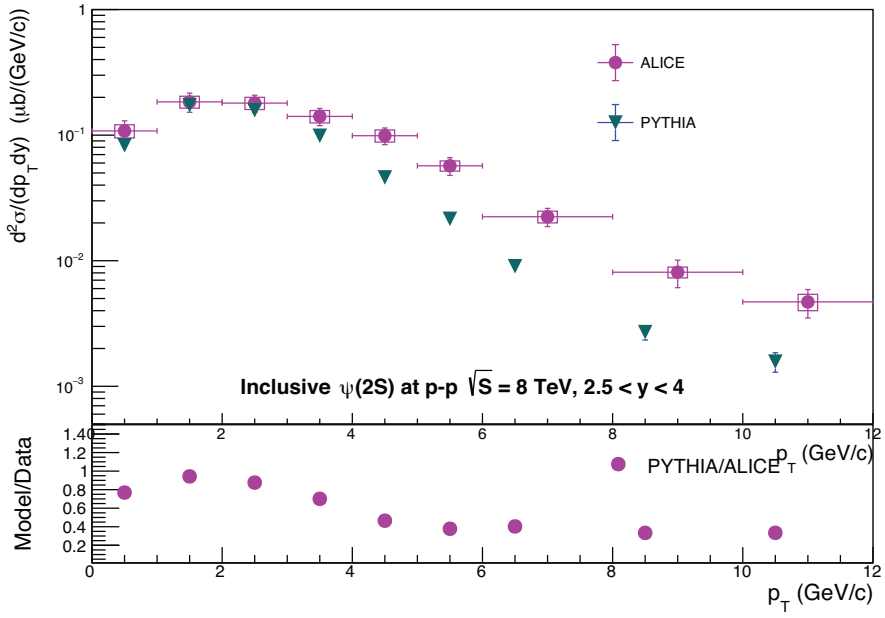

Figure 7. The p_T distribution for the differential cross-section of $\psi(2S)$ production in pp collisions at $\sqrt{s} = 8$ TeV.

3.4. J/ψ resonance at $\sqrt{s} = 8$ TeV

In Figure 9, J/ψ differential cross-section distribution is shown in the p_T interval from 020 GeV/c. Ten million events are generated for J/ψ. The differential cross-section distribution obtained from the simulated result is compared with the ALICE [19] and LHCb measurements [22] (the bottom panel shows the ratio of the yields for data coming from the model to the experiments). We can see that initially, simulated yield of J/ψ is approximately same as published data of experiments up to 4.0 GeV/c in p_T, after that simulated data underestimate the experimental data thus the ratios decreases linearly with p_T.

In Figure 10, the differential cross-section of J/ψ is shown in y bins from 2.54. Five million pp events are generated for J/ψ. The measured differential cross-section of simulated result is compared with the measurement performed by ALICE and LHCb collaborations (the bottom panel shows the ratio of the yields for simulated data from the model to the data from both experiments). It seems that initially, simulated yield of J/ψ is similar to the ALICE published result up to 3.1 in y, after that a continuous discrepancy is observed in yield and the model overestimate the experimental data. LHCb distributions are lower again as compared to ALICE data and PYTHIA simulated data.

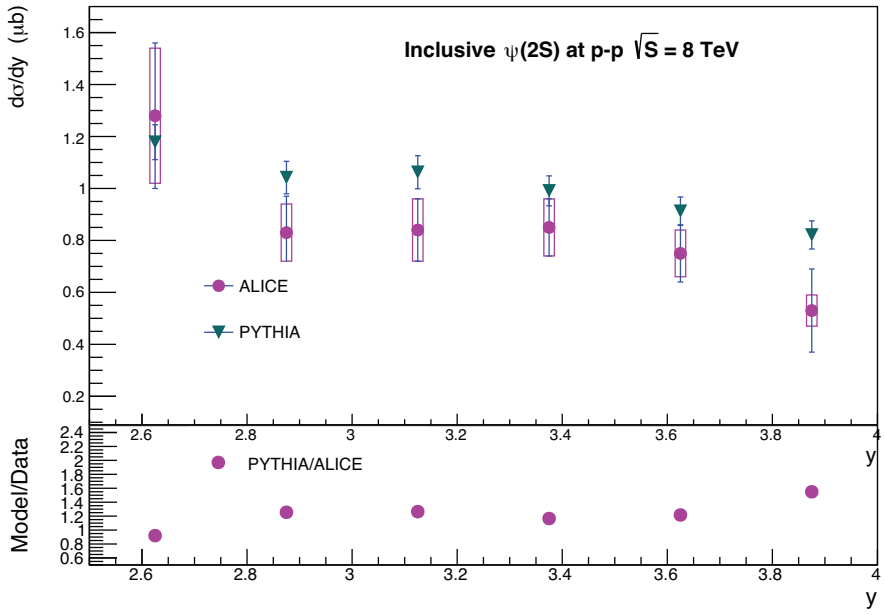

Figure 8. The y distribution for the differential cross-section of $\psi(2S)$ production in pp collisions at $\sqrt{s} = 8$ TeV.

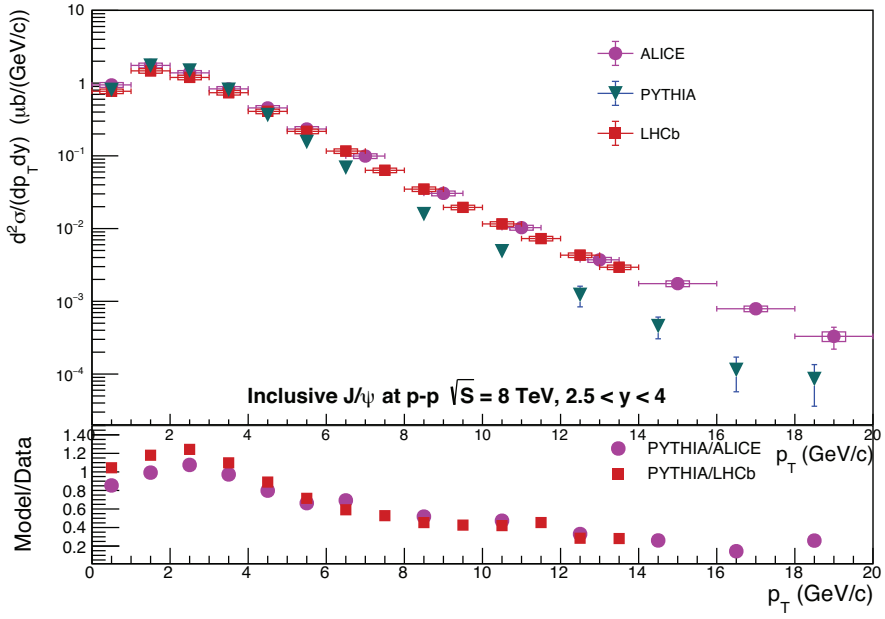

Figure 9. The p_T distributions for the differential cross-section of J/ψ production in pp collisions at $\sqrt{s} = 8$ TeV.

3.5. Ratio of $\psi(2S)$ to J/ψ cross-section at $\sqrt{s} = 8$ TeV

The ratio of inclusive $\psi(2S)$ to J/ψ cross-section is plotted as a function of p_T and y at $\sqrt{s} = 8$ TeV. The ratio is calculated using the results generated by PYTHIA8 model for $\psi(2S)$ and J/ψ. The obtained ratio is compared with ALICE data. The cross-section ratio of $\psi(2S)$ over J/ψ as function of p_T is shown in Figure 11. Most likely at low $p_T < 2\ GeV/c$ the ratio calculated is similar to the experimental one, however at higher p_T in the interval of $2 < p_T < 12\ GeV/c$ the experimental data distribution is systematically higher than

simulated distribution. The cross-section ratio of $\psi(2S)$ over J/ψ as function of y is shown in Figure 12. The cross-section ratio calculated from simulated result is compared with the published ALICE measurement [19]. The y dependent pattern of simulated result is close to our expectation and similar to the published results.

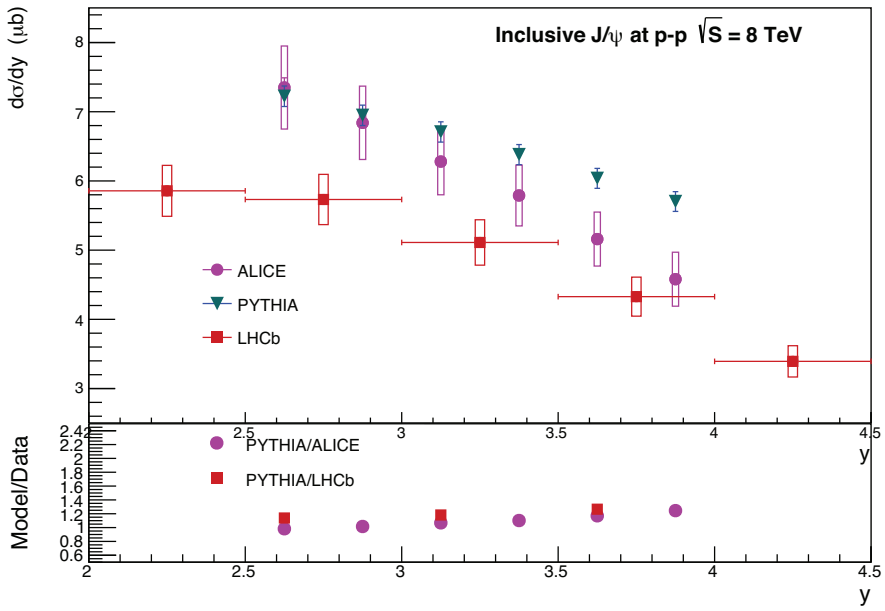

Figure 10. The y distributions for the differential cross-section of J/ψ production in pp collisions at $\sqrt{s} = 8$ TeV.

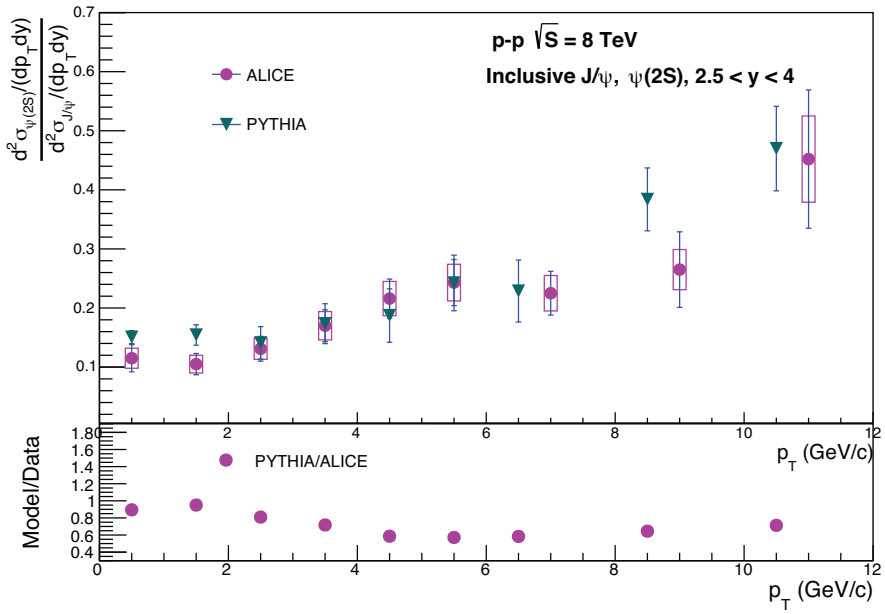

Figure 11. The y distribution for the differential cross-section of J/ψ production in pp collisions at $\sqrt{s} = 8$ TeV.

3.6. $\psi(2S)$ Resonance at $\sqrt{s} = 7$ TeV

The production cross-section of inclusive $\psi(2S)$ in pp collision at $\sqrt{s} = 7$ TeV and forward rapidity range of $2.5 < y < 4$, as a function of p_T and y is simulated using PYTHIA 8, compared to the previously published

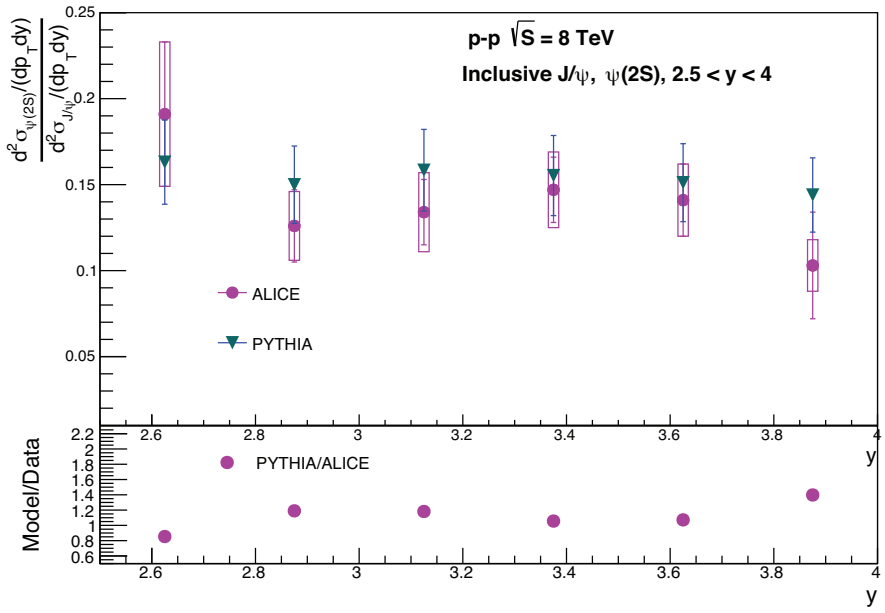

Figure 12. The y distributions for the differential cross-section of J/ψ production in pp collisions at $\sqrt{s} = 8$ TeV.

ALICE [20] and LHCb results [23] in the mentioned p_T and y ranges of $0 < p_T < 12$ GeV/c and $2.5 < y < 4$ respectively. Figure 13 shows the differential cross-section of $\psi(2S)$. Ten million events are generated for $\psi(2S)$. The measured differential cross-section from simulated result is compared with the published ALICE [20] and LHCb measurements [23]. The bottom panel shows the ratio of the yields. One can see that very different behavior is observed as a function of p_T. In the interval of $p_T = 3.5$ GeV/c (I interval), the model's predictions are similar to the ALICE and LHCb distribution; in the interval of $p_T > 3.5$ (region II) the simulated distribution is lower than the ALICE and LHCb data. In Figure 14, the differential cross-section of $\psi(2S)$ is shown in y bins from 2.54. About five million pp events are generated for $\psi(2S)$. The distribution of differential cross-section obtained from model is compared with the measurement performed by ALICE and LHCb collaborations (the bottom panel shows the ratio of the yields). We can see that the model can well describe the ALICE experimental data only for y = 2.6 and y = 3.9, while for other values the PYTHIA8 underestimate the ALICE data, while LHCb distribution is lower compared to the simulated distribution and ALICE experimental data distribution.

3.7. J/ψ resonance at $\sqrt{s} = 7$ TeV

The differential cross-section of inclusive J/ψ in pp collision at $\sqrt{s} = 7$ TeV, as a function of p_T and y in forward rapidity range of $2.5 < y < 4$ is simulated using PYTHIA 8 and compared with previously published ALICE results. In Figure 15, the differential cross-section of J/ψ is shown in p_T from 020 GeV/c. Ten million events are generated for J/ψ. The measured differential cross-section from simulated result is compared with the published ALICE and LHCb measurements. The bottom panel shows the ratio of the yields. Again like the data from the previous section one can say that there are 2 p_T regions for the behavior of the p_T distributions: region I for the $p_T = 3$ GeV/c; region II for the $p_T > 4$ GeV/c. In region I with p_T the ratio is constant, in region II, it decreases sharply, showing the deviation of simulation as compared to both experimental data distributions.

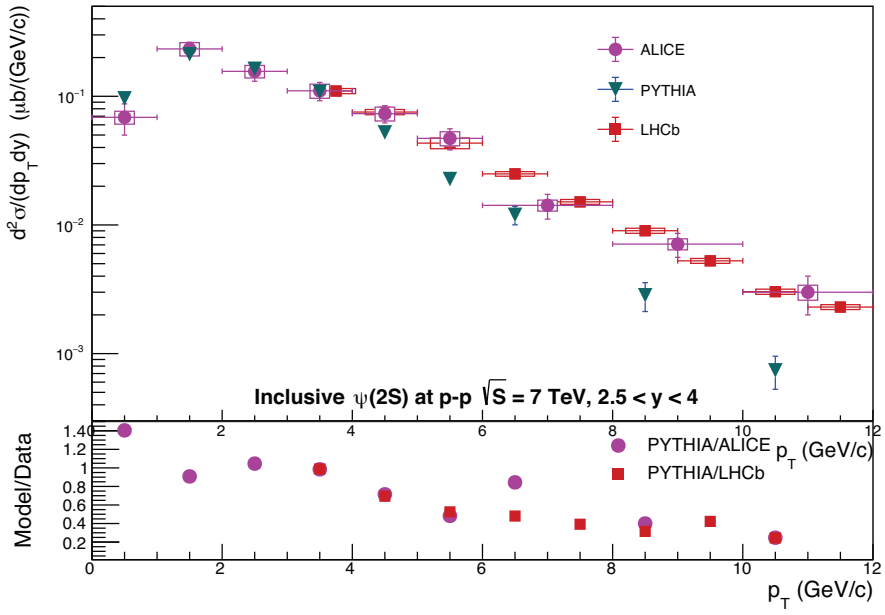

Figure 13. The p_T distributions for the differential cross-section of $\psi(2S)$ production in pp collisions at $\sqrt{s} = 7$ TeV. The bottom panel shows the ratio of the yields.

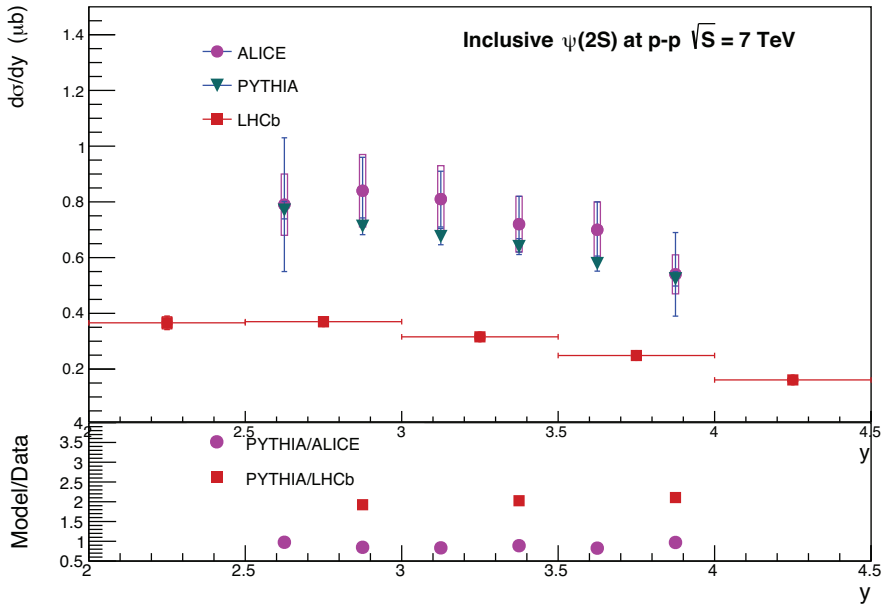

Figure 14. The y distributions for the differential cross-section of $\psi(2S)$ production in pp collision.

In Figure 16, the differential cross-section of J/ψ is shown in y bins from 2.54. Five million pp events are generated for J/ψ. The simulated differential cross-section is compared to the measurement performed by ALICE and LHCb collaboration (the bottom panel shows the ratio of the yields). It appears that the ratio is around 1 for the interval of $y < 2.6$ and increase at the values of y out of the interval. Thus model seems to overestimate both the ALICE and LHCb data.

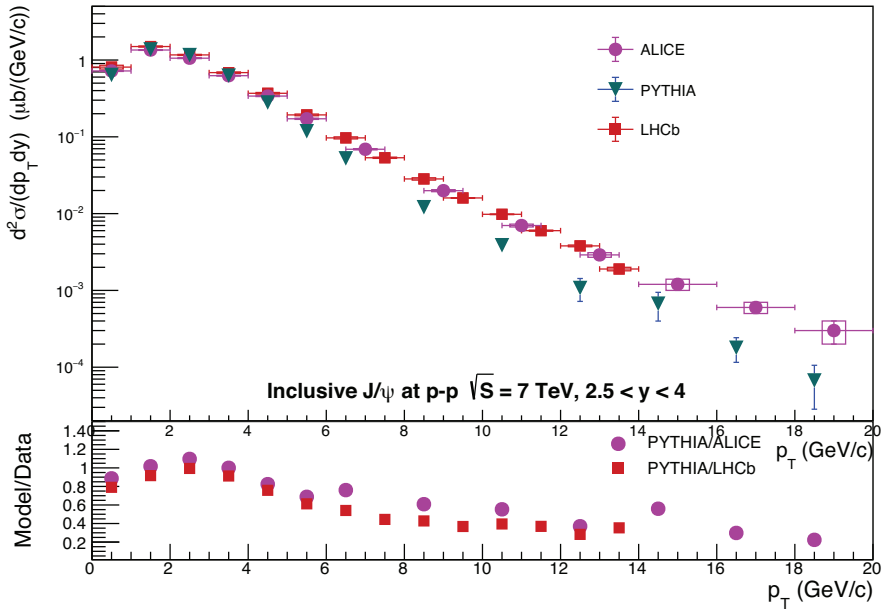

Figure 15. The p_T distributions for the differential cross-section of J/ψ production in pp collisions at $\sqrt{s} = 7$ TeV.

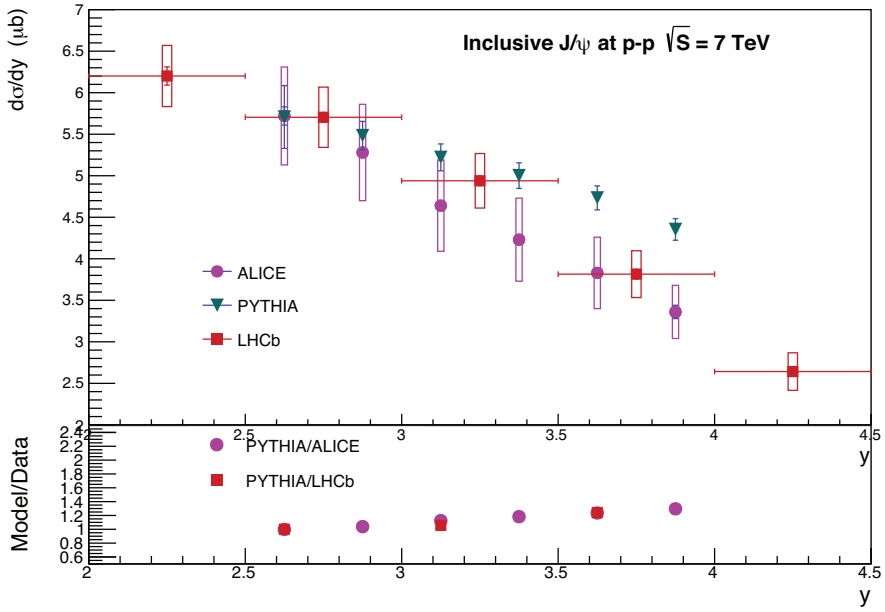

Figure 16. The y distributions for the differential cross-section of J/ψ production in pp collisions at $\sqrt{s} = 7$ TeV.

3.8. Ratio of $\psi(2S)$ to J/ψ cross-section at $\sqrt{s} = 7$ TeV

The ratio of inclusive $\psi(2S)$ to J/ψ cross-section is plotted as a function of p_T and y at $\sqrt{s} = 7$ TeV, and is calculated using the results generated by PYTHIA 8 model for $\psi(2S)$ and J/ψ. The calculated ratio is compared with ALICE published ratio.

The cross-section ratio of $\psi(2S)$ over J/ψ as function of p_T is shown in Figure 17. The cross-section ratio calculated from simulated result is compared with the published ALICE measurement. The p_T dependent pattern of simulated result is close to our expectation and similar to experimental results moreover increases

linearly with p_T. Similar behavior was observed for pp collision at $\sqrt{s} = 13$ TeV. The cross-section ratio of $\psi(2S)$ over J/ψ as function of y is shown in Figure 18. The cross-section ratio calculated from simulated result is compared with the published ALICE [20] and LHCb measurements [21, 23]. The y dependent pattern of simulated result is again close to our expectation and similar to the published results and again matched with the behavior at $\sqrt{s} = 8$ and 13 TeV; however, the distribution does not depend on y. Again the LHCb distribution is lower compared to the simulated distribution and ALICE experimental data distribution.

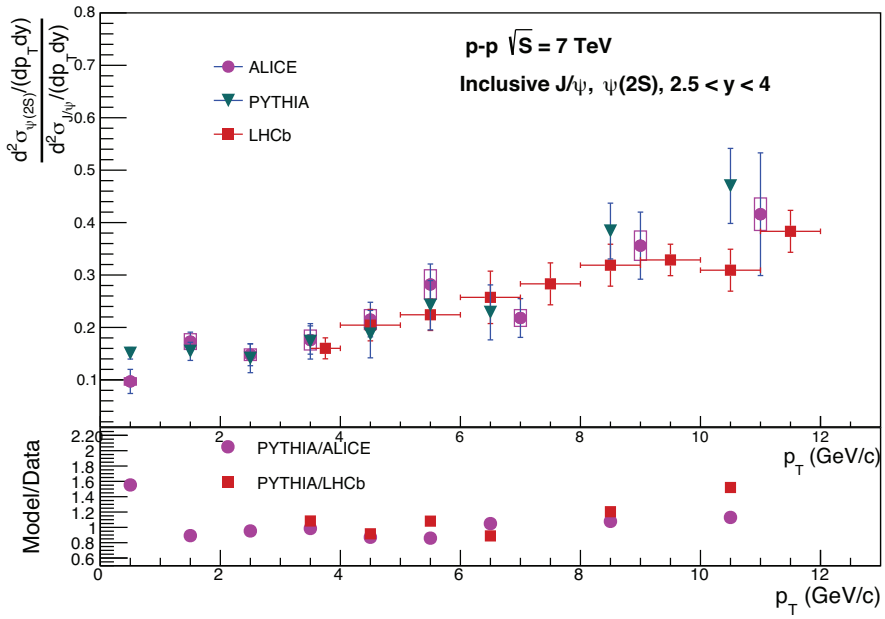

Figure 17. The p_T dependence of ratios for the differential cross-section of $\psi(2S)$ productions to ones for the J/ψ productions.

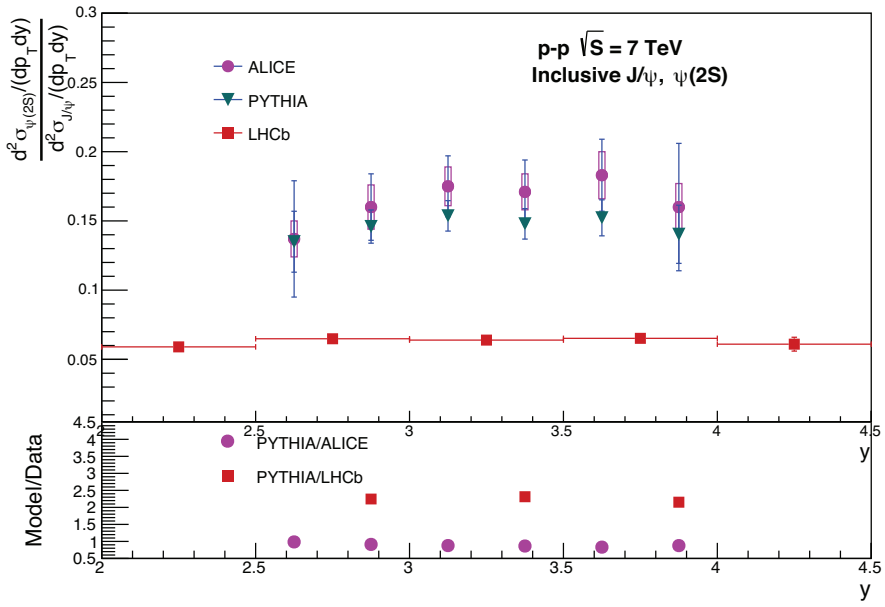

Figure 18. The y dependence of ratios for the differential cross-section of $\psi(2S)$ productions to ones for the J/ψ productions.

4. Conclusion

The obtained results give possibility to say that the PYTHIA 8 model:

1. Gives good predictions for the soft part (low p_T interval) of p_T distributions of J/ψ and $\psi(2S)$ but the predictions are lower than the experimental data for the hard part of the distributions, the boundary values of the interval depend on energy.

2. Model's predictions are in good agreement with the ALICE data in the y interval close to midrapidity region, while with increase in the y interval, the predictions overestimate the experimental data. The boundary values of the interval depend on energy.

3. Can explain well the ratios of inclusive cross-sections of $\psi(2S)$ production to ones for J/ψ productions as a function of p_T and y.

4. At all energies considered in the analysis, LHCb differential cross-section distributions of J/ψ and $\psi(2S)$ plotted as a function of y are lower compared to the ALICE data and PYTHIA simulated distributions.

References

[1] Campbell J, Huston J, Krauss F. The Black Book of Quantum Chromodynamics: A Primer for the LHC Era. Oxford, UK: Oxford University Press, 2018, pp. 1-749.

[2] Peter BM, Jochen W. The phase diagram of strongly-interacting matter. Review of Modern Physics 2009; 81: 1031-1050.

[3] Huston J, Rabbertz K, Zanderighi G. Quantum chromodynamics. In: Tanabashi M, Hagiwara K, Hikasa K, Nakamura K, Sumino Y et al. Review of Particle Physics: Particle Data Groups. Physical Review D 2018 (update 2019); 98: 1-54.

[4] Harald F. Producing heavy quark flavors in hadronic collisions: a test of quantum chromodynamics. Physics Letters B 1977; 67 (2): 217-221.

[5] Amundson JF, Eboli OJP, Gregores EM, Halzen F. Quantitative tests of color evaporation: charmonium production. Physics Letters B 1997; 390: 323-328.

[6] Geoffrey TB, Eric B, George PL. Rigorous QCD analysis of inclusive annihilation and production of heavy quarkonium. Physical Review D 1995; 51: 1125-1171.

[7] Xiaojian D, Ralf R. $\psi(2S)$ production at the LHC. Journal of Physics Conference Series 2016; 779 (1).

[8] Yan L, Zhuang P, Xu N. J/ψ production in quark-gluon plasma. Physical Review Letters 2006; 97: 232301.

[9] CMS Collaboration. J/ψ and $\psi(2S)$ production in pp collisions at $\sqrt{s} = 7$ TeV. Journal of High Energy Physics 2012; 2: 011.

[10] Lucas A. Charmonium production in pp collisions with ALICE at the LHC. In: International Conference on High Energy Physics (ICHEP 2018); Seoul, Korea; 2019. p. 040.

[11] Biswarup P. Inclusive $\psi(2S)$ production at forward rapidity in pp,p-Pb and Pb-Pb collisions with ALICE at the LHC. In: 7th International Conference on Physics and Astrophysics of Quark Gluon Plasma (ICPAQGP 2015); Kolkata, India; 2017. p. 043.

[12] ALICE Collaboration. Inclusive J/ψ production at mid-rapidity in pp collisions at $\sqrt{s} = 5.02$ TeV. Journal of High Energy Physics 2019; 10: 084.

[13] Louis K, Helmut S. Color deconfinement and charmonium production in nuclear collisions. Landolt-Bornstein Group Elementary Particles, Nuclei and Atoms 2010; 23: 373.

[14] Peter BM, Johanna S. Charmonium from statistical hadronization of heavy quarks – a probe for deconfinement in the quark-gluon plasma. Landolt-Bornstein 2010; 23: 424.

[15] Kari JE, Petja P, Hannu P, Carlos AS. EPPS16: Nuclear parton distributions with LHC data. Europen Physical Journal C 2017; 77 (3): 163.

[16] Karol K, Aleksander K, Tomas J, David BC, Cynthia K. nCTEQ15 - Global analysis of nuclear parton distributions with uncertainties in the CTEQ framework. Physical Review D 2016; 93 (8): 085037.

[17] Chun LH. Recent results on heavy flavor in small and large systems from ALICE. Proceeding of LHCP 2020 Conference 2020; 036.

[18] Shreyasi A. Energy dependence of forward-rapidity J/ψ and $\psi(2S)$ production in pp collisions at the LHC. European Physical Journal C 2017; 77 (6): 392.

[19] ALICE Collaboration. Inclusive quarkonium production at forward rapidity in pp collisions at $\sqrt{s}$ = 8 TeV. European Physical Journal C 2016; 76: 184.

[20] ALICE Collaboration. Measurement of quarkonium production at forward rapidity in pp collisions at $\sqrt{s}$ = 7 TeV. European Physical Journal C 2014; 74 (8): 2974.

[21] Calvo Gómez M, Camboni A, Vilasís Cardona X, LHCb Collaboration - CERN. Measurement of $\psi(2S)$ production cross-sections in proton-proton collisions at $\sqrt{s}$ = 7 and 13 TeV. European Physical Journal C 2020; 80 (3): 185.

[22] Aaij R, Abellan Beteta C, Adeva B, Adinolfi M, Adrover C et al. Production of J/ψ and Upsilon mesons in pp collisions at $\sqrt{s}$ = 8 TeV. Journal of High Energy Physics 2013; 6: 064.

[23] Aaij R, Adeva B, Adinolfi. Measurement of J/ψ production in pp collisions at $\sqrt{s}$ =7 TeV. The European Physical Journal C 2011; 71: 1645.

[24] Torbjörn S, Stefan A, Jesper RC, Richard C, Nishita D et al. An introduction to PYTHIA 8.2. Computer Physics Communications 2015; 191: 159-177.

[25] Torbjorn S, Stephen M, Peter ZS. A brief introduction to PYTHIA 8.1. Computer Physics Communications 2008; 178 (11): 852-867.

[26] Torbjorn S, Maria VZ. A multiple interaction model for the event structure in hadron collisions. Physical Review D 1987; 36: 2019.

[27] Torbjorn S, Peter ZS. Multiple interactions and the structure of beam remnants. Journal of High Energy Physics 2004; 3: 053.

[28] Spyros A, Torbjorn S. Effects of color reconnection on $t\bar{t}$ final states at the LHC. Journal of High Energy Physics 2014; 11: 043.

[29] Bo A, Gosta G, Gunnar I, Torbjorn S. Parton fragmentation and string dynamics. Physics Reports 1983; 97: 31-145.